Journal of Alloys and Compounds 509S (2011) S141–S144

Contents lists available at ScienceDirect

Journal of Alloys and Compounds

journal homepage: www.elsevier.com/locate/jallcom

Topological instability and glass forming ability of Al–Ni–Sm alloys

L.C.R. Aliaga, G.P. Danez, C.S. Kiminami, C. Bolfarini, W.J. Botta*

Departamento de Engenharia de Materiais, Universidade Federal de São Carlos, Rodovia Washington Luiz, km 235, 13565-905, São Carlos, SP, Brazil

ARTICLE INFO

Article history:
Received 25 August 2010
Received in revised form
23 December 2010
Accepted 5 January 2011
Available online 12 January 2011

Keywords:
Crystallization
Al-based alloys
Glass forming ability
λ criterion
Amorphous alloys

ABSTRACT

The thermal crystallization of Al-based metallic glasses can be described in association with the topological instability λ criterion. In the present work, we report on the crystallization behavior and glass forming ability of Al-rich, Al–Ni–Sm alloys, designed with compositions corresponding to the same topological instability condition of $\lambda \approx 0.1$. Amorphous melt-spun alloys were prepared with the following compositions, varying the ratio of Ni and Sm elements: $Al_{87.5}Ni_4Sm_{8.5}$, $Al_{83.5}Ni_{10}Sm_{6.5}$, $Al_{80.5}Ni_{14.5}Sm_5$ and $Al_{76.5}Ni_{20.5}Sm_3$. The glass forming ability of each alloy composition was evaluated based on the thermal parameters obtained from DSC runs and on X-ray diffraction patterns. Better glass forming ability was observed in compositions whose Sm content was increased and Ni content reduced. Thermal crystallization of the alloys with low Sm content showed only one crystallization peak and no glass transition event. In alloys with higher rare-earth content, a glass transition event was clearly detected before the crystallization event. The results are interpreted considering the different types and proportions of Sm–Al and Ni–Al clusters that can be formed in the alloys along the $\lambda \approx 0.1$ line. They also emphasize the relevance of these different types of clusters in the amorphous phase in defining the stability of the glass and the types of thermal crystallization.

1. Introduction

The concept of topological instability first proposed in 1984 [1] has been used to explain different aspects of metallic amorphous alloys, such as their glass forming ability and the stability of supercooled liquid. The original topological instability criterion, the λ-criterion, offered a satisfactory explanation of the compositional range of binary Al-based systems to form amorphous alloys. The inclusion of the λ-criterion in multicomponent systems was also successful in predicting the thermal behavior of Al–TM–RE (TM, transition metal and RE, rare-earth element) alloys [2]. This criterion proved able to identify alloy compositions which, upon continuous heating, exhibit a supercooled liquid region (defined as glassy alloys, with $\lambda > 0.1$), nanocrystalline behavior (defined as nanocrystalline alloys, with $\lambda < 0.1$) or an intermediate behavior, where nanocrystallization is preceded by a supercooled liquid region (defined as nano-glassy alloys, with $\lambda \approx 0.1$).

The validity of the correlation between the λ-criterion and crystallization behavior has been confirmed in many multicomponent Al-based systems, such as Al–Y–RE–Ni–Co [3], Al–Y–Gd [4], Al–Y–Ni–Co–Sc [5], Al–Ni–La [6], Al–Y–Ni–Co–Pd [7] and others [8]. In all evaluated systems, an increment in the value of the λ parameter has resulted in a clear transition from nano-crystallization to glassy behavior, usually with some degree of stabilization of the supercooled liquid. However, contrary to the expected behavior, the best glass former composition in each system is consistently found to be a nano-glassy and off-eutectic composition with $\lambda \approx 0.1$ [9].

In the case of other systems such as Cu–Zr–Al [10], Cu–Zr–Ti [11], Cu–Hf–Al [12] and Ca–Mg–Zn [13] with high glass forming ability, experimental evidence suggests that the best glass former compositions are the ones showing glassy behavior during crystallization with values of $\lambda > 0.1$. Furthermore, extensive results of the critical cooling rate for overcoming crystal nucleation, the T_g/T_m ratio and the maximum sample thickness for fully amorphous structures [14] in many alloy systems strongly support this correlation between the easy-glass former composition and the system's glassy behavior during crystallization. Taking this observation into account, together with the λ-criterion for compositions with λ higher than 0.1, we suggest that a correlation also exists between the λ values of a given alloy and its glass forming ability [15].

Recent studies of molecular dynamics simulations in binary systems have demonstrated that it is possible for the atoms to be arranged to form different types of coordination polyhedra or quasi-equivalent clusters in the same alloy [16], in the context of "soft" atoms. Also, other thermodynamics computational studies have shown the influence of the elastic constants in increasing the Gibbs free energy of solid solutions or intermetallic compounds, thus favoring the stabilization of the supercooled liquid or the amorphous phase.

---

* Corresponding author. Tel.: +55 16 33518553; fax: +55 16 33615404.
E-mail address: wjbotta@ufscar.br (W.J. Botta).

0925-8388/$ – see front matter © 2011 Elsevier B.V. All rights reserved.
doi:10.1016/j.jallcom.2011.01.026

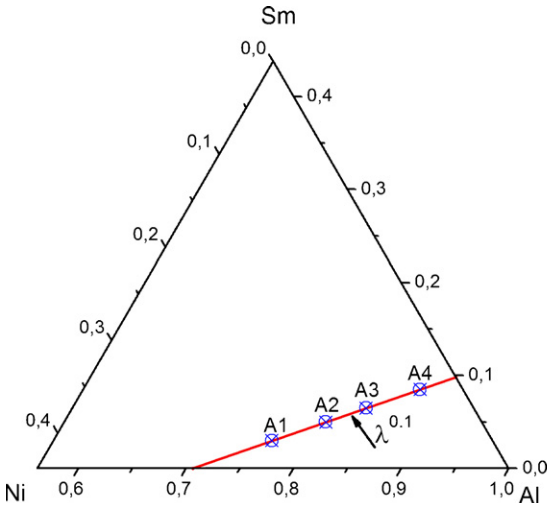

Fig. 1. Alloy compositions and position in the compositional triangle of the Al–Ni–Sm system. The transversal line is the $\lambda \approx 0.1$ line. (A1) $Al_{76.5}Ni_{20.5}Sm_3$, (A2) $Al_{80.5}Ni_{14.5}Sm_5$, (A3) $Al_{83.5}Ni_{10}Sm_{6.5}$, and (A4) $Al_{87.5}Ni_4Sm_{8.5}$.

In the present study, we examined the crystallization behavior and glass forming ability of Al-rich, Al–Ni–Sm alloys designed with compositions corresponding to the same topological instability condition of $\lambda \approx 0.1$. Sm was chosen as the rare-earth alloying element due to its high values of volumetric and shear modulus, which can be also correlated with an improvement in the GFA of alloys.

2. Experimental procedure

Four Al-rich Al–Ni–Sm alloys were designed with compositions corresponding to the same topological instability condition of $\lambda \approx 0.1$, as indicated in the composition triangle represented in Fig. 1. The samples with nominal compositions of $Al_{87.5}Ni_4Sm_{8.5}$, $Al_{83.5}Ni_{10}Sm_{6.5}$, $Al_{80.5}Ni_{14.5}Sm_5$ and $Al_{76.5}Ni_{20.5}Sm_3$ were prepared by a two-step process. Bulk ingots were produced from a mixture of high purity elements by repeatedly arc-melting to ensure complete melting and compositional homogeneity in a water-cooled copper crucible in a Ti-getter argon atmosphere.

Amorphous ribbons were then produced from the ingots, using a single-roller melt spinner at a tangential wheel speed of 40 m/s in argon atmosphere. The approximate width and thickness of the melt-spun ribbons were 3 mm and 40 μm.

The samples were structurally characterized by standard X-ray diffraction (XRD) in the reflection mode, using Cu-K_α radiation. The phase transformation temperatures during heating were studied by differential scanning calorimetry (DSC) at a heating rate of 0.67 K/s.

3. Results and discussion

Fig. 2 shows the DSC curves corresponding to the four as-prepared ingots, whose peaks correspond to the melting process of each alloy on the *liquidus* temperature (T_l). The occurrence of multiple endothermic peaks indicates that the alloys are off-ternary eutectic compositions; moreover, the volumetric fraction of each phase differs in each alloy.

Fig. 3 shows the XRD patterns of the four alloys, all of which show a broad peak confirming the formation of amorphous phase. However, as the ratio Ni/Sm increased, the presence of crystalline phases became more evident, and in fact, the $Al_{76.5}Ni_{20.5}Sm_3$ alloy with the lowest Sm content displayed a clear peak corresponding to a non-identified crystalline phase.

Fig. 4 shows the corresponding DSC curves for the same group of alloys. Decreasing the Ni/Sm ratio (increasing Sm content from 3 at.% to 8 at.%) caused a change in the crystallization behavior, as already observed in other Al-based amorphous alloys with compositions along the $\lambda \approx 0.1$ line [17,18]. A glass transition (T_g) event was not detected in the alloy containing 3 at.% Sm; however, a clear glass transition temperature was observed in the alloys containing 5 at.%, 6.5 at.% and 8.5 at.% Sm, indicating that the type of atomic organization changes as the proportion of rare-earth element increases.

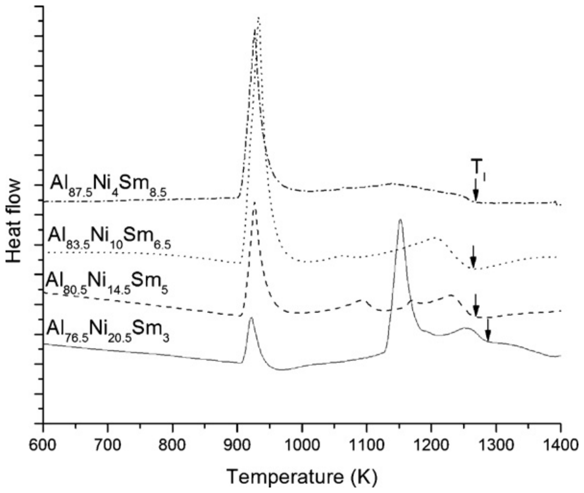

Fig. 2. DCS curves from as prepared ingots of each alloy.

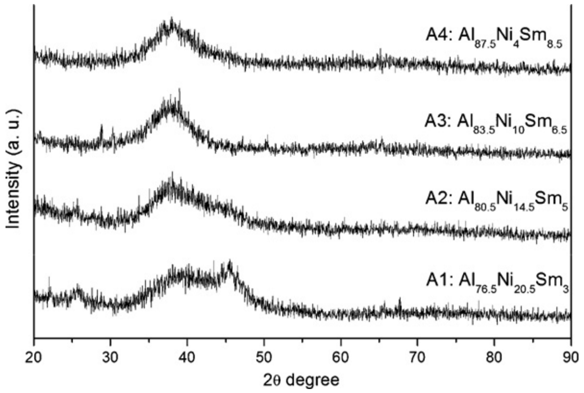

Fig. 3. X-ray diffraction patterns of Al-based ribbons in the as-quenched state.

Table 1 summarizes the thermal parameters obtained from the DSC curves for the Al–Ni–Sm alloys. The glass stability, as indicated by the crystallization temperatures (T_x) and glass transition temperatures, clearly increases as the Ni/Sm ratio increases, although,

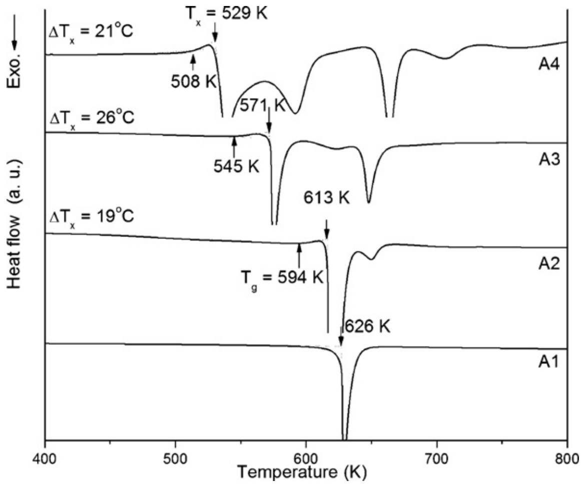

Fig. 4. DSC scans at a heating rate of 0.67 K s^{-1} of the as-quenched ribbons.

Table 1
Thermal parameters of melt-quenched ribbons.

Alloy	T_g (K)	T_x (K)	T_l (K)	T_{rg}	ΔT_x (K)
$Al_{76.5}Ni_{20.5}Sm_3$	–	626	1282	–	–
$Al_{80.5}Ni_{14.5}Sm_5$	594	613	1279	0.464	19
$Al_{83.5}Ni_{10}Sm_{6.5}$	545	571	1268	0.429	26
$Al_{87.5}Ni_4Sm_{8.5}$	508	529	1268	0.401	21

as mentioned earlier, no glass transition temperature was observed in the alloy with the highest Ni content.

The different crystallization behaviors observed in alloys with compositions corresponding to the value of $\lambda \approx 0.1$ found in this work and in other systems [18,19] cannot be explained based solely on the concept of topological instability. Topological aspects associated with cluster configurations in the supercooled liquid should also be taken into account to justify the differences in crystallization behavior. The cluster arrangements in Al-based alloys can change depending on the relative amount of rare-earth elements and transition metals. Also, the relative fraction of the different types of clusters has already been associated with the glass transition phenomenon.

The change in the nature of atomic bonding from the covalent to the metallic type has already been observed in many Al–TM–RE alloys compositions, in association with the type of coordinating atom. In fact, Sheng et al. [16] have shown that the average coordination number changes with the effective atomic size, and this parameter is directly dependent on the alloy's atomic composition.

In the Al–Ni–Sm ternary alloy system, the atomic radii of Al, Ni and Sm are: $R_{Al} = 0.1432$ nm, $R_{Ni} = 0.1246$ nm, and $R_{Sm} = 0.1810$. Considering the radius ratio between Al, Sm and Ni, one finds the following ratios:

$$\frac{R_{Sm}}{R_{Al}} = 1.2642 \quad \text{and} \quad \frac{R_{Ni}}{R_{Al}} = 0.8701$$

In the first case, the ratio between R_c, the radius of the central atom, and R_e, the radius of the outer atom, $R = R_c/R_e = 1.2642$, which favors the formation of clusters with the coordination number $Nc = 17$, and in the second case, $R = 0.8701$ and the $Nc = 11$ cluster may be formed.

According to the efficient cluster packing model, the ideal ratio for the first cluster is 1.248 [20] and for the second one it is 0.884. However, this second type of cluster is not so common in the structure of glassy metals since they are the most unstable ones. Clusters with $Nc = 11$ and $Nc = 12$ are topologically nearly identical [21] and thus the $Nc = 11$ clusters are not expected to form in favor of the more efficiently packed icosahedra. In addition, icosahedral symmetric clusters have the lowest free energy up to a size of 5000 atoms [22] evidencing their higher stability.

Considering yet the atoms like hard spheres, from the following expression [23] it is possible to determine the surface packing factor of the cluster, and thus to determine how open are the clusters structure.

$$\eta_{2D} = \frac{Nc}{2}\left(1 - \frac{\sqrt{R_c^2 + 2R_eR_c}}{R_c + R_e}\right) \quad (1)$$

In expression (1) η_{2D} is the surface packing factor, Nc is a coordination number and R_c and R_e have been defined previously.

Considering $Nc = 17$ for the first type of cluster and $Nc = 11$ for the second type, we obtain $\eta_{2D} = 0.8726$ in the case of the Sm centered cluster and $\eta_{2D} = 0.6315$ in the case of the Ni centered cluster. These results suggest that the Ni centered clusters have a more open structure and are therefore more easily deformed or destroyed.

We can also argue that the value of the surface energy, as low as possible, is relevant in organizing the external shape of crystals. The same concept can also be applied for clusters; it is likely that the stability of the clusters are associated with a minimum in the surface energy, in which case there would be tendency for the $Nc = 11$ to stabilize as icosahedral cluster with $Nc = 12$.

Although all compositions are located on and along the $\lambda = 0.1$ line, they display distinct behaviors because their local topology is not the same, i.e., in principle, Ni-rich compositions have a larger number of unstable clusters with $Nc = 11$ and only a minor fraction of $Nc = 17$ clusters.

In this configuration, the glass transition event is not perceptible in the thermal behavior, as was the case of the $Al_{76.5}Ni_{20.5}Sm_3$ alloy. When the Sm content is increased, some of the Ni atoms are substituted by Sm atoms, leading to a corresponding change in the cluster configuration from coordination number 11 to 12. In this case, the glass transition event can be detected in the DSC thermograms. Moreover, the thermal stability of alloys with $\lambda = 0.1$ reaches its optimal condition in the presence of the highest number of icosahedral clusters in the alloy structure.

It is important to note that the center of the XRD halo is displaced to higher angles, indicating the presence of a larger number of closely packed clusters in the amorphous structure [24].

On the other hand, in compositions richer in Sm, the main type of clusters will be $Nc = 17$ clusters. Although this type of cluster is very common in the glassy structure, its stability is not as high as the $Nc = 12$ cluster, and therefore the thermal stability of the alloys is expected to decrease, as was observed in the $Al_{87.5}Ni_4Sm_{8.5}$ alloy. In alloys with even higher Sm content, thermal crystallization occurs with no detection of the glass transition temperature.

This interpretation of our results complements the topological instability parameter in describing the crystallization behavior of Al-based alloys, mainly for compositions in the central region of the Al-rich corner in Al–TM–RE systems.

Studies on $Al_{85}Ni_{10}Ce_5$, $Al_{87}Ni_{10}Ce_3$ [25,26], $Al_{90}Fe_xCe_{10-x}$ ($x = 3, 5, 7$) [27–30], $Al_{87}Y_8Ni_5$, $Al_{90}Y_{10}$ [31], $Al_{100-2x}Co_xCe_x$ ($x = 8, 9, 10$) and $Al_{80}Fe_{10}Ce_{10}$ [32] have indicated the existence of two distinct basic structural cluster units, RE/Al and TM/Al, in Al–TM–RE systems. The number of these units with respect to the Al content is undoubtedly relevant in determining the thermal behavior during crystallization.

Similar studies of the Al–Ni–La system [18] have shown that the glass transition event is associated with RE/Al clusters and that a critical concentration of these unities is necessary in the supercooled liquid for a good detection of T_g.

RE–Al clusters show lower thermal stability against crystallization than TM–Al clusters, as evidenced in $Al_{90}Fe_5Ce_5$ alloys [33], in which Fe/Al clusters were detected after the onset of crystallization, as well as in $Al_{85}Ni_{10}Ce_5$ and $Al_{87}Ni_{10}Ce_3$ alloys [31], in which Ni/Al clusters were detected after the first crystallization stage.

Considering the soft atoms model, i.e., the atoms like a soft spheres leading to a more realistic structures packing, it is possible to establish a correlation between the volumetric modulus of the RE and TM elements and the stability of the clusters; for instance, Ni has higher volumetric modulus than Sm and thus Ni centered clusters must show stronger stability when the $Nc = 12$ configuration is reached. This is in fact reflected in the stability of the supercooled liquid region, although the detection of the glass transition event is dependent on a critical concentration of RE/Al clusters.

4. Conclusions

The topological instability λ criterion was applied to select amorphous alloy compositions in the Al–Ni–Sm system and evaluate the effect of the relative amounts of transition metal and rare-earth elements on the glass forming ability.

Although all alloy compositions are located on and along the $\lambda = 0.1$ line, i.e., with the same topological instability, they show different thermal crystallization behaviors.

In the alloys containing larger amounts of rare-earth elements, a clear glass transition event was detected and was associated with the stability of clusters with coordination number $Nc = 17$. In the alloys containing more transition metal elements, associated with the formation of $Nc = 11$ unstable clusters, the glass transition event could not be detected. The stability of the supercooled liquid is associated with $Nc = 12$ TM/Al clusters.

Acknowledgments

The authors would like to thank FAPESP, CNPq and CAPES for financial support.

References

[1] T. Egami, Y. Waseda, J. Non-Cryst. Solids 64 (1984) 113.
[2] R.D. Sá Lisboa, C. Bolfarini, W.J. Botta F., C.S. Kiminami, Appl. Phys. Lett. 86 (2005) 211904.
[3] D.V. Louzguine, A. Inoue, J. Light Met. 1 (2001) 105.
[4] F.Q. Guo, S.J. Poon, G. Shiflet, Mater. Sci. Forum 331–337 (2000) 31.
[5] D.V. Louzguine, S. Sobu, A. Inoue, Appl. Phys. Lett. 85 (2004) 3758.
[6] K.L. Sahoo, M. Wollgarten, J. Haug, J. Banhart, Acta Mater. 53 (2005) 3861.
[7] D.V. Louzguine-Luzgin, A. Inoue, J. Alloys Compd. 399 (2005) 78.
[8] D.V. Louzguine-Luzgin, A. Inoue, W.J. Botta, Appl. Phys. Lett. 88 (2006) 011911.
[9] B. Idzikowsky, P. Sveck, M. Miglierini, Properties and Applications of Nanocrystalline Alloys from Amorphous Precursors, in: NATO Science Series, 2001.
[10] D. Wang, H. Tan, Y. Li, Acta Mater. 53 (2005) 2969.
[11] Z.P. Lu, H. Bei, C.T. Liu, Intermetallics 15 (2007) 618.
[12] P. Jia, H. Guo, Y. Li, J. Xu, E. Ma, Scripta Mater. 54 (2006) 2165.
[13] O.N. Senkov, J.M. Scott, D.B. Miracle, J. Alloys Compd. 424 (2006) 394.
[14] A. Inoue, Acta Mater. 48 (2000) 279.
[15] C.S. Kiminami, R.D. SáLisboa, M.F. de Oliveira, C. Bolfarini, W.J.F. Botta, Mater. Trans. JIM 48 (2007) 1739.
[16] H.W. Sheng, W.K. Luo, F.M. Alamgir, J.M. Bai, E. Ma, Nature Vol.439 (2006) 419.
[17] O.N. Senkov, D.B. Miracle, H.M. Mullens, J. Appl. Phys. 97 (2005) 103502.
[18] W.J. Botta, C. Triveño Rios, R.D. Sá Lisboa, A.R. de Andrade, M.F. de Oliveira, C. Bolfarini, C.S. Kiminami, J. Alloys Compd. 483 (2009) 89.
[19] P. Gargarella, C.S. Kiminami, M.F. de Oliveira, C. Bolfarini, W.J. Botta, J. Alloys Compd. 495 (2010) 334.
[20] D.B. Miracle, Acta Mater. 54 (2006) 4317.
[21] T. Egami, V. Levashov, R. Aga, J.R. Morris, Metall. Mater. Trans. A 39 (2008) 1786.
[22] A.L. Mackay, J.L. Finney, K. Gotoh, Acta Cryst. A 33 (1977) 98.
[23] S. Cozzini, M. Ronchetti, Phys. Rev. B 53 (1996) 12040.
[24] M. Stoica, K. Hajlaoui, J. Das, J. Eckert, A.R. Yavary, Rev. Adv. Mater. Sci. 18 (2008) 61.
[25] M. Matsuura, M. Sakurai, K. Suzuki, A.P. Tsai, A. Inoue, Mater. Sci. Eng. A 226–228 (1997) 511.
[26] M. Matsmira, M. Sakurai, S.H. Kim, A.P. Tsai, A. Inoue, K. Suzuki, Mater. Sci. Eng. A 217–218 (1996) 397.
[27] H.Y. Hsieh, T. Egami, Y. He, S.J. Poon, G.J. Shiflet, J. Non-Crystall. Solids 135 (1991) 248.
[28] H.Y. Hsieh, B.H. Toby, T. Egami, Y. He, S.J. Poon, G.J. Shiflet, J. Mater. Res. 5 (1990) 2807.
[29] A.N. Mansour, G. Cibin, A. Marcelli, T. Sevastyanova, G. Yalovega, A.V. Soldatov, J. Synchrotron Radiat. 8 (2001) 809.
[30] A.N. Mansour, A. Marcelli, G. Cibin, G. Yalovega, T. Sevastyanova, A.V. Soldatov, Phys. Rev. B 65 (2002) 134207-1.
[31] M. Matsuura, Zeitschrift für Naturforschteil 44A (1989) 814.
[32] A.N. Mansour, C.P. Wong, R.A. Brizzolara, Phys. Rev. B 50 (1994) 12401.
[33] L. Zhang, K. Chen, X. Huang, Y. Wu, X. Bian, J. Phys.: Condens. Matter 13 (2001) 5947.